Ionics (2018) 24:83–89
DOI 10.1007/s11581-017-2189-4

ORIGINAL PAPER

Enhanced electrochemical performances of Li_2MnO_3 cathode materials by Al doping

Yanhong Xiang[1,2] · **Xianwen Wu**[2,3]

Received: 17 April 2017 / Revised: 28 May 2017 / Accepted: 8 June 2017 / Published online: 24 June 2017

Abstract Al-doped Li_2MnO_3 ($Li_2Mn_{0.9}Al_{0.1}O_3$) lithium-rich layered oxide is prepared and investigated as cathode material for lithium-ion batteries (LIBs). X-ray diffraction (XRD) and scanning electron microscopy-energy dispersive spectrometer (SEM-EDS) analyses reveal that the Al element is distributed in the sample homogenously. The Al-LMO sample exhibits a great improvement on the rate capability and cycling stability compared to the LMO sample. The differential capacity versus voltage (dQ/dV) results reveal that Al doping would be to prevent the first charge phase transformation from a layered phase to a cubic spinel-like phase and also slowdown the rate of transformation upon cycling. Electrochemical impedance spectroscopy (EIS) results confirm that Al doping decreases the charge-transfer resistance and improves the electrochemical reaction kinetics.

Keywords Li_2MnO_3 · Sol-gel · Lithium-ion battery · Cathode material · Al

✉ Yanhong Xiang
112301009@csu.edu.cn

[1] School of Physics, Mechanical & Electrical Engineering, Jishou University, Jishou, Hunan 416000, China

[2] The Collaborative Innovation Center of Manganese-Zinc-Vanadium Industrial Technology (the 2011 Plan of Hunan Province), Jishou, Hunan 416000, China

[3] School of Chemistry and Chemical Engineering, Jishou University, Jishou, Hunan 416000, China

Introduction

LIBs have been widely used in electric vehicles, energy storage power stations, and portable electronic devices (such as mobile phones, laptop computers, digital cameras, etc.) [1–3]. The demands for the next-generation LIBs with higher energy density have increased in terms of capacity, voltage, safety, and cost [4–9]. Lithium intercalation compounds based on manganese oxides are cheaper, safer, and less toxic than the layered compound based on cobalt or nickel oxides and, therefore, offer a particularly attractive replacement for the latter compound as a cathode material in LIBs [10–13]. Among the lithium manganese oxides cathode materials studied, spinel oxides ($LiMn_2O_4$), layered oxides ($LiMnO_2$), and Li-rich Mn-based layered compounds ($Li_2MnO_3{\cdot}LiMO_2$ (M = Mn, Ni, Co)) cathodes have been proposed and widely investigated [14–20]. The implementation of the spinel oxide $LiMn_2O_4$ has been delayed because of relatively low theoretical capacity (148 mAh g^{-1}), limited storage, and cycling performances at elevated temperatures [21, 22]. Layered $LiMnO_2$ compounds have come to be of interest as cathode material because of their high theoretical capacity (285 mAh g^{-1}), but layered $LiMnO_2$ is not thermodynamically stable, which is easily converted to a spinel-like structure during electrochemical extraction/insertion of Li ions [23]. Recently, Li-rich Mn-based layered compounds have been considered as one of the most promising cathode material for future LIBs because of their advantage of high reversible capacity (>200 mAh g^{-1}) when charged above 4.5 V [24–27].

A common feature of Li-rich Mn-based layered compound cathode is an irreversible high voltage plateau at around 4.5 V vs Li/Li^+ during the first charge. Li_2MnO_3 is the end member of these materials which exhibits the

characteristic first-charge plateau around 4.5 V [28–30]. Initial discharge capacity values of this materials are generally high after activation of Li_2MnO_3 phase, but cycling instability and intrinsically inferior rate capability are observed in all reports [11, 31, 32]. Therefore, it would be beneficial to reinvestigate the properties of Li_2MnO_3 material to help further understanding of the properties of Li-rich Mn-based layered compounds. In this manuscript, Al-doped sample $Li_2Mn_{0.9}Al_{0.1}O_3$ (Al-LMO) and pristine Li_2MnO_3 (LMO) materials are synthesized by a sol-gel method. The structural and electrochemical properties of the synthesized materials are investigated.

Experimental

The sol-gel method was adopted to prepare the Al-LMO and LMO samples using citric acid as the chelating agent: Stoichiometric amounts of $LiCH_3COO{\cdot}2H_2O$, $Mn(CH_3COO)_2{\cdot}4H_2O$, and $Al(NO_3)_3{\cdot}9H_2O$ (Al-LMO) were dissolved in distilled water to achieve a mixture of 2.0 mol L^{-1} metal solution. Then, an aqueous solution of citric acid (2.0 mol L^{-1}) was added to the above aqueous solution with constant magnetic stirring. The resultant solution was evaporated at 80 °C under vigorous stirring to get a viscous gel. Next, the resulting gel was dried at 120 °C for 12 h. Finally, the gathered precursor was heated to 450 °C for 6 h and calcined at 950 °C for 12 h under air atmosphere to obtain the target material.

X-ray diffraction (XRD) measurement of material was recorded on a Rigaku 2500 X-ray diffractometer using Cu-Kα radiation. The diffraction data was collected over the range of $10° < 2\theta < 80°$. The morphology of the powder was investigated by scanning electron microscopy (SEM, TESCAN, MAIA3). For the electrochemical characterization, the positive electrodes for the cells were prepared by mixing active material with polyvinylidene difluoride (PVDF) binder and carbon black in a weight ratio of 8:1:1 in *N*-methyl-2pyrrolidone (NMP) solvent. Then, the slurry was cast onto an Al foil current collector and subsequently dried at 105 °C for 10 h in air. The laminates were cut into disks (14 mm) and dried under vacuum at 65 °C for 6 h. The electrochemical tests were carried out using coin-type cells which consisted of a cathode and a lithium metal anode separated by a polyethylene/polypropylene film (Celgard 2400). Cells were assembled in an argon-filled glove box with the electrolyte of 1 mol/L $LiPF_6$-EC/DMC/DEC (1:1:1 by volume). The charge-discharge tests were operated on a LAND-CT2001A battery test equipment (Jinnuo Wuhan Co. Ltd., P.R. China) at room temperature. Electrochemical impedance spectroscopy (EIS) was carried out on an electrochemical workstation (CHI660E, Shanghai Chenhua) in the frequency range from 0.1 MHz to 0.01 Hz.

Results and discussion

The XRD patterns of the LMO and Al-LMO samples are shown in Fig. 1. All the major peaks in each pattern can be indexed to the layered structure with a C2/m space group [33, 34]. The superlattice peaks between 20° and 30° in the XRD profiles, which are characteristic of Li-rich Mn-based layered compounds, are due to Li/Mn cation arrangement in the transitional metal (TM) layers [35]. No impurity peak is detected in XRD patterns of Al-LMO sample due to the low quantity of the doping. In addition, the intensity of superlattice peak between 20° and 30° is reduced by Al-doping, indicating that the Li/Mn ordering in the TM layer is disrupted by Al-doping.

SEM micrographs of the LMO and Al-LMO samples are presented in Fig. 2a. The morphology of samples has not changed clearly with Al doping. As can be seen, the primary particles (300–400 nm) of the LMO and Al-LMO samples agglomerate with each other and form secondary particles. The EDS images of Al-LMO sample (Fig. 2b) confirm that the Al element is uniformly distributed in the sample.

The Li_2MnO_3 phase is originally considered to be electrochemically inactive because the oxidation state of Mn ion is +4 and it is not expected to be oxidized to higher oxidation state. However, it is now well established that Li can be electrochemically extracted and reinserted. Many researchers attributed the electrochemical activity of Li_2MnO_3 phase to the removal of Li_2O from the active material [30, 36], and another researchers found that proton exchange (exchange Li^+ by H^+) might have contributed to such an anomalous phenomenon [37]. Figure 3 shows the first charge/discharge curves of the LMO and Al-LMO cathodes. The charge/discharge process is

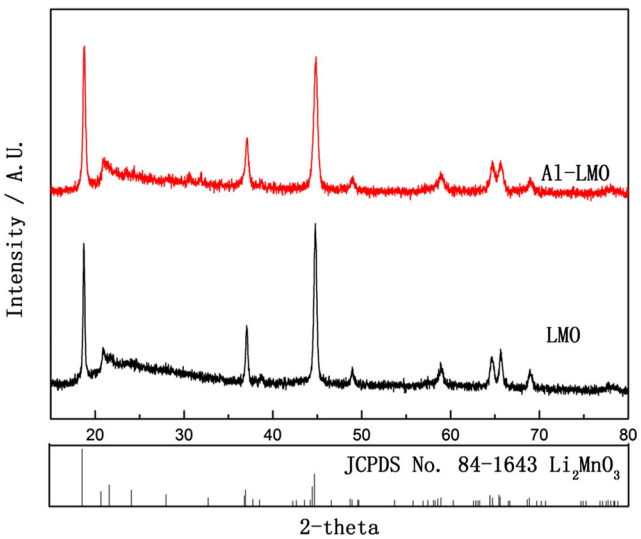

Fig. 1 X-ray diffraction patterns of the pristine Li_2MnO_3 (LMO) and Al-doped Li_2MnO_3 (Al-LMO) samples

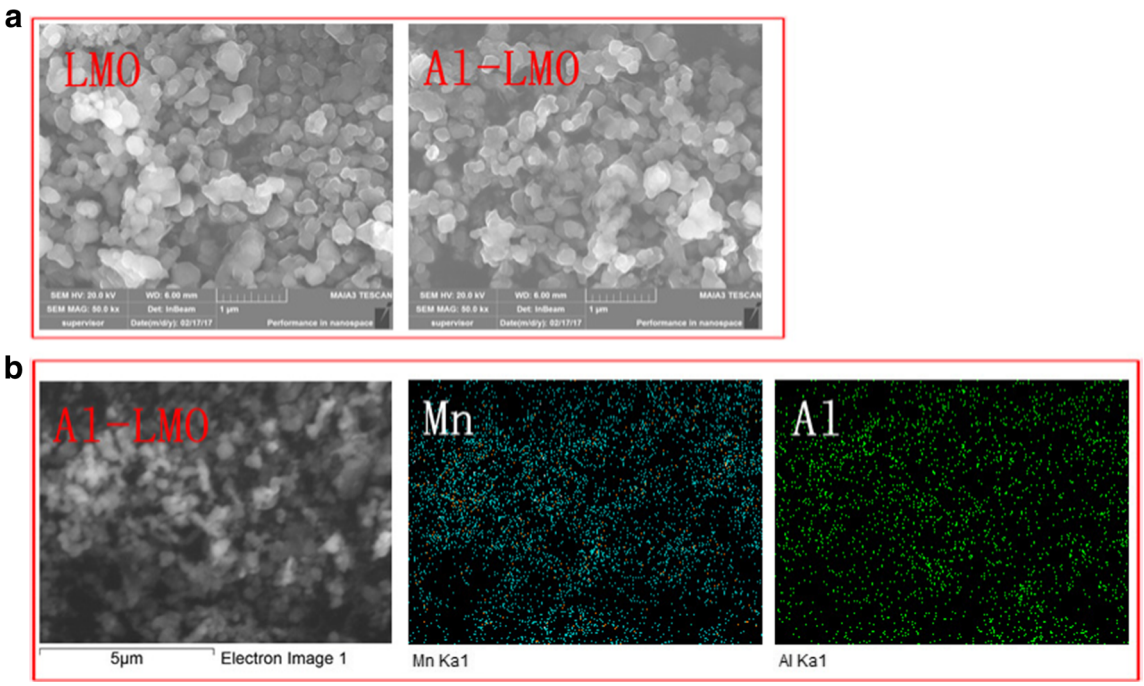

Fig. 2 **a** The SEM images of the pristine Li_2MnO_3 (LMO) and Al-doped Li_2MnO_3 (Al-LMO) samples. **b** The EDS images of the Al-LMO sample

operated in the voltage range from 2.0 to 4.8 V at 0.05 C (12.5 mA g^{-1}), which is low enough to ensure a quasistatic process. A classic platform feature of Li-rich Mn-based cathode materials at 4.5 V is observed for all samples' initial charge curves. The initial discharge capacities of LMO and Al-LMO samples are 122 and 99 mAh g^{-1}, and the first cycle efficiency (FCE) is 50 and 58.9% for LMO and Al-LMO samples, respectively. It can be obviously observed that the Al-LMO sample delivered a lower charge/discharge capacity but a higher FCE than the LMO sample. The decrease of capacities can be attributed to the stronger Al-O bond (comparing to Li-O bond) which can suppress the exaction of Li_2O from Li_2MnO_3 component during the first activation [38].

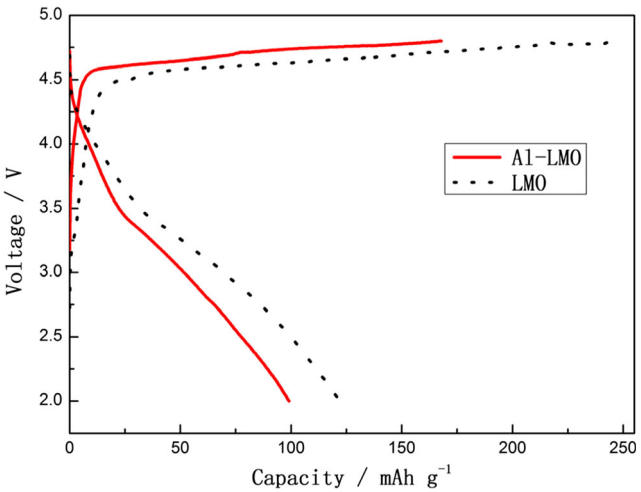

Fig. 3 Charge/discharge profiles of the pristine Li_2MnO_3 (LMO) and Al-doped Li_2MnO_3 (Al-LMO) samples

The differential capacity versus voltage (dQ/dV) plots corresponding to the 1st, 2nd, 3rd, and 10th cycles of samples are collected and shown in Fig. 4. The oxidation reaction of LMO and Al-LMO cathodes can be characterized by two main peaks around 4.6 and 4.7 V, which are related with the removal of Li_2O from the active material Li_2MnO_3 component or proton exchange [28, 30]. It can be found from Fig. 4a that there are two oxidation peaks at 3.3 and 3.7 V in the initial charge process for the LMO sample. These phenomena indicate that the layered phase transformed to the cubic spinel-like phase with the LMO sample in the initial charge process [39]. Compared to the LMO sample, these two oxidation peaks at 3.3 and 3.7 V are not observed in the initial charge process for the Al-LMO sample, which implied that Al doping would prevent the first charge phase transformation. A main broad reduction peak at 3.4 V, which can be attributed to the lithiation of the layered active MnO_2 into layered $LiMnO_2$ [40], is observed in the initial discharge process for LMO and Al-LMO samples. During subsequent discharges (Fig. 4b, c), the reduction of Mn^{4+} in the layered active MnO_2 component that occurs initially at ~3.4 V also shifts to lower potentials but increases in magnitude toward ~2.8 V, characteristic of a lithium manganese oxide spinel-like phase [40]. Additionally, the oxidation

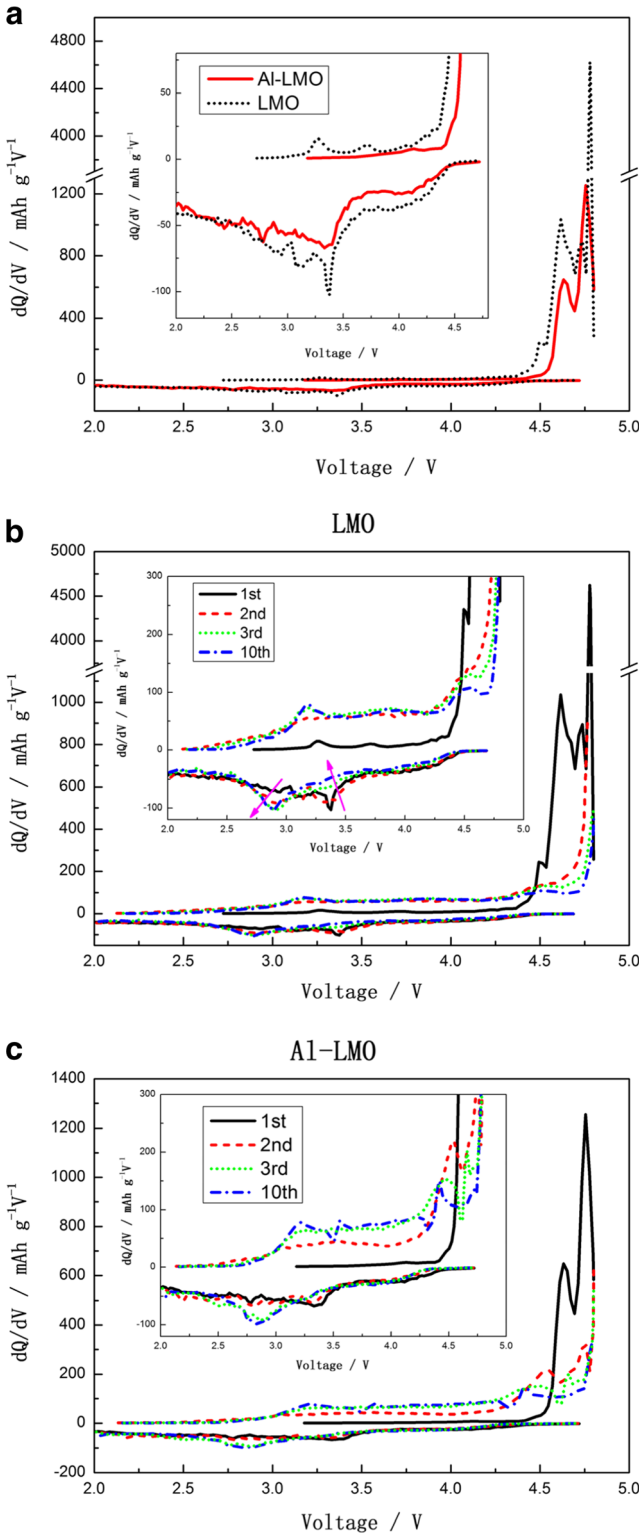

Fig. 4 Differential capacity versus voltage (dQ/dV) for cells of the pristine Li_2MnO_3 (LMO) and Al-doped Li_2MnO_3 (Al-LMO) samples in the voltage range of 2.0–4.8 V. **a** The initial dQ/dV curves for LMO and Al-LMO samples. **b** The dQ/dV curves for LMO sample. **c** The dQ/dV curves for Al-LMO sample

peaks around 3.3 V appeared slowly upon cycling by the Al-LMO sample from Fig. 4c, which indicates that Al doping would slowdown the rate of cubic spinel-like phase transformation of layered phase and thus implies excellent cycle stability.

To further investigate the Al-doped effects on the electrochemical properties of the sample, the electrodes are cycled at different rates (0.05, 0.1, 0.2, 0.5, 1.0, 2.0 C) between 2 and 4.8 V. Figure 5 shows the rate capabilities of the LMO and Al-LMO samples. When the electrodes are cycled at high rates up to 2.0 C and then returned to 0.1 C, the low rate capacities are returned to the initial value, which revealed that cycling at high rates (0.2, 0.5, 1.0, 2.0 C) did not have any adverse effect on the low rate (0.1 C) capacity. It can be obviously observed that the rate capacities of Al-LMO sample are higher than LMO sample. The electrode of Al-LMO sample cycled at 2.0 C rate exhibited about 31.2% capacity retention as compared to 1.8% for LMO sample with regard to the capacity obtained at 0.05 C rate, which indicates that Al-LMO sample has perfect electrical conductivity than LMO sample.

Figure 6 shows the cycle performances of the LMO and Al-LMO samples at 0.1 C between 2.0 and 4.8 V at room temperature. It can be obviously observed that Al-LMO sample behaves better than LMO sample: an initial discharge capacity of 99.4 mAh g^{-1} with capacity retention of 97.1% after 40 cycles for the former but only 84 mAh g^{-1} with 84.8% for the latter.

It is expected that the conducting Li ions can move to the neighboring positions more easily when the Mn^{4+} ions are replaced by low-valence cations [29]. To verify the improvement in electrochemical performances of the Al-LMO sample shown above, EIS of LMO and Al-LMO

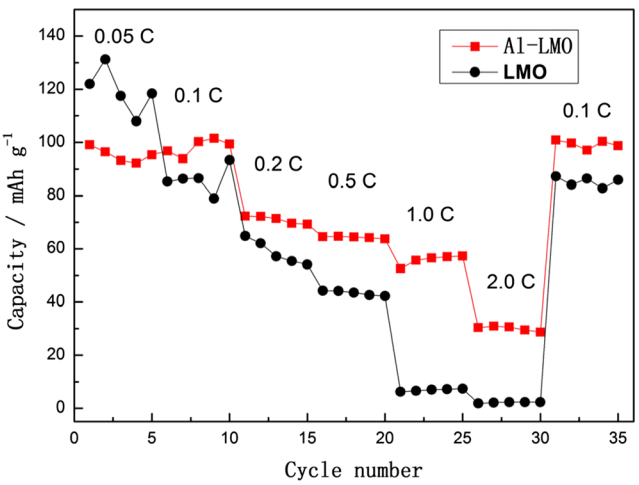

Fig. 5 Rate capability of the pristine Li_2MnO_3 (LMO) and Al-doped Li_2MnO_3 (Al-LMO) samples at 0.05, 0.1, 0.2, 0.5, 1.0, and 2.0 C rate

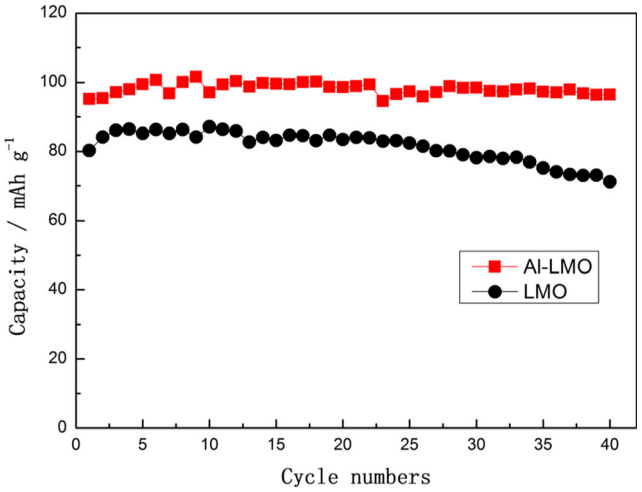

Fig. 6 Cycling performance of the pristine Li_2MnO_3 (LMO) and Al-doped Li_2MnO_3 (Al-LMO) samples at 0.1 C between 2.0 and 4.8 V at room temperature

samples are collected after 40 cycles. Figure 7 shows the Nyquist plots and the corresponding equivalent circuit. The plots of the two electrodes are well fitted with the equivalent circuit. In the equivalent circuit, R_e, R_f, R_{ct}, and W1 represent the resistance of liquid electrolyte, the resistance of the SEI film, the charge-transfer resistance, and the Warburg impedance of lithium ion diffusion, respectively [41–43]. It is found that Al-LMO sample has a relatively lower R_{ct} (5185 Ω) compared with LMO sample (10,037 Ω). The decrease in R_{ct} demonstrated that Al-doping can improve both the electronic conductivity and the Li^+ diffusion during insertion/extraction [44, 45], which is also supported by the rate capability and charge/discharge cycling data.

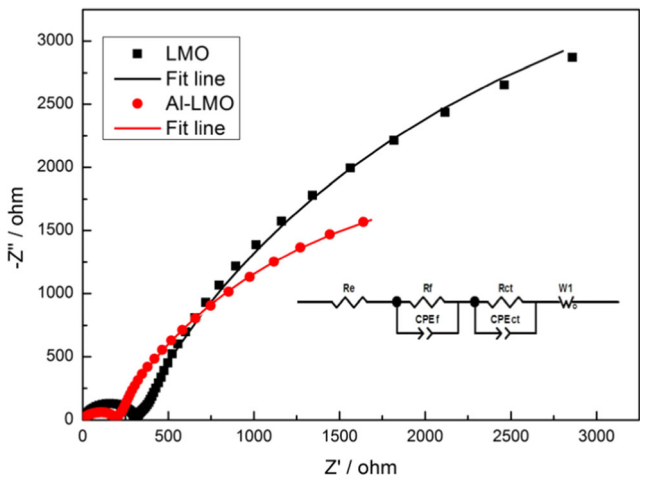

Fig. 7 Nyquist plots of the pristine Li_2MnO_3 (LMO) and Al-doped Li_2MnO_3 (Al-LMO) samples after 40 cycles

Conclusions

The pristine LMO and Al-LMO cathode materials for lithium-ion battery are synthesized through the conventional sol-gel method. Its structure, morphology, and electrochemical properties are investigated in this work. All the major peaks in each XRD pattern can be indexed to the layered structure with a C2/m space group. SEM-EDS (SEM-EDS) analyses revealed that the Al element is distributed in the sample homogenously. The electrochemical behavior of cycled LMO and Al-LMO samples indicates the phase transformation from a layered to a spinel. The Al-LMO sample exhibited a great improvement on cycle and rate performances compared to the LMO sample. The dQ/dV results show that Al doping would prevent the phase transformation in the first charge process and slowdown the rate of spinel phase transformation of layered phase in the following cycles. EIS results confirm that Al doping decreases the charge-transfer resistance and improves the electrochemical reaction kinetics.

Acknowledgements The work was supported by the National Natural Science Foundation of China (Nos. 51662010, 51364009, 51262008, 51472107, and 51672104), the National Natural Science Foundation of Hunan Province, China (No. 2016JJ6121), the Educational Commission of Hunan Province, China (Nos. 16B209 and 16B190), the Research Startup Foundation of Jishou University (No. jsdxrcyjkyxm201409), the Collaborative Innovation Center of Manganese Zinc Vanadium Industrial Technology (the 2011 Plan of Hunan Province), the Research Foundation of Jishou University of Hunan Province, China (Nos. JDLF2016010, 15JDY024, JDSTLY1503, JDZ201503, 2015 [20] and JDST201508), the Aid program (Environment and Energy Materials and deep processing of mineral resources in Wuling Mountain) for Science and Technology Innovative Research Team in Higher Educational Institutions of Hunan Province (2014[107]), and the Planned Science and Technology Project of Science and Technology Bureau of Xiangxi Tujia & Miao Autonomous Prefecture.

References

1. Croy JR, Abouimrane A, Zhang Z (2014) Next-generation lithium-ion batteries: the promise of near-term advancements. MRS Bull 39:407–415
2. Dunn B, Kamath H, Tarascon JM (2011) Electrical energy storage for the grid: a battery of choices. Science 334:928–935
3. Goodenough JB (2014) Electrochemical energy storage in a sustainable modern society. Energy Environ Sci 7:1–14
4. Wang J, Liu Z, Yan G, Li H, Peng W, Li X, Song L, Shih K (2016) Improving the electrochemical performance of lithium vanadium fluorophosphate cathode material: focus on interfacial stability. J Power Sources 329:553–557
5. Amine K, Kanno R, Tzeng Y (2014) Rechargeable lithium batteries and beyond: progress, challenges, and future directions. MRS Bull 39:395–401
6. Tarascon JM, Armand M (2001) Issues and challenges facing rechargeable lithium batteries. Nature 414:359–367
7. Sun YK, Myung ST, Park BC, Prakash J, Belharouak I, Amine K (2009) High-energy cathode material for long-life and safe lithium batteries. Nat Mater 8:320–324

8. Wang J, Li X, Wang Z, Huang B, Wang Z, Guo H (2014) Nanosized $LiVPO_4F$/graphene composite: a promising anode material for lithium ion batteries. J Power Sources 251:325–330
9. Wang J, Zhang Q, Li X, Xu D, Wang Z, Guo H, Zhang K (2014) Three-dimensional hierarchical Co_3O_4/CuO nanowire heterostructure arrays on nickel foam for high-performance lithium ion batteries. Nano Energy 6:19–26
10. Wang D, Wang X, Yu R, Bai Y, Wang G, Liu M, Yang X (2016) The control and performance of $Li_4Mn_5O_{12}$ and Li_2MnO_3 phase ratios in the lithium-rich cathode materials. Electrochim Acta 190:1142–1149
11. Yan J, Liu X, Li B (2014) Recent progress in Li-rich layered oxides as cathode materials for Li-ion batteries. RSC Adv 4:63268–63284
12. Zhong S, Hu P, Luo X, Zhang X, Wu L (2016) Preparation of $LiNi_{0.5}Mn_{1.5}O_4$ cathode materials by electrospinning. Ionics 22: 2037–2044
13. Wu L, Lu J, Wei G, Wang P, Ding H, Zheng J, Li X, Zhong S (2014) Synthesis and electrochemical properties of xLiMn$_{0.9}$Fe$_{0.1}$PO$_4$·yLi$_3$V$_2$(PO$_4$)$_3$/C composite cathode materials for lithium-ion batteries. Electrochim Acta 146:288–294
14. Wang Z, Wang Z, Guo H, Peng W, Li X (2015) Synthesis of Li_2MnO_3-stabilized $LiCoO_2$ cathode material by spray-drying method and its high-voltage performance. J Alloy Compd 626: 228–233
15. Liu Y, Zhang Z, Fu Y, Wang Q, Pan J, Su M, Battaglia VS (2016) Investigation the electrochemical performance of $Li_{1.2}Ni_{0.2}Mn_{0.6}O_2$ cathode material with $ZnAl_2O_4$ coating for lithium ion batteries. J Alloy Compd 685:523–532
16. Chen M, Chen D, Liao Y, Zhong X, Li W, Zhang Y (2016) Layered lithium-rich oxide nanoparticles doped with spinel phase: acidic sucrose-assistant synthesis and excellent performance as cathode of lithium ion battery. ACS Appl Mater Inter 8:4575–4584
17. Zhao Y, Xia M, Hu X, Zhao Z, Wang Y, Lv Z (2015) Effects of Sn doping on the structural and electrochemical properties of $Li_{1.2}Ni_{0.2}Mn_{0.8}O_2$ Li-rich cathode materials. Electrochim Acta 174:1167–1174
18. Johnson CS, Korte SD, Vaughey JT, Thackeray MM, Bofinger TE, Shao-Horn Y, Hackney SA (1999) Structural and electrochemical analysis of layered compounds from Li_2MnO_3. J Power Sources 81-82:491–495
19. He L, Xu J, Han T, Han H, Wang Y, Yang J, Wang J, Zhu W, Zhang C, Zhang Y (2017) $SmPO_4$-coated $Li_{1.2}Mn_{0.54}Ni_{0.13}Co_{0.13}O_2$ as a cathode material with enhanced cycling stability for lithium ion batteries. Ceram Int 43:5267–5273
20. Wang R, Li X, Wang Z, Guo H, Wang J (2015) Electrochemical analysis for cycle performance and capacity fading of lithium manganese oxide spinel cathode at elevated temperature using p-toluenesulfonyl isocyanate as electrolyte additive. Electrochim Acta 180:815–823
21. Wang R, Li X, Wang Z, Guo H (2015) Manganese dissolution from $LiMn_2O_4$ cathodes at elevated temperature: methylene methanedisulfonate as electrolyte additive. J Solid State Electr 20: 19–28
22. Wang R, Li X, Wang Z, Guo H, Hou T, Yan G, Huang B (2015) Lithium carbonate as an electrolyte additive for enhancing the high-temperature performance of lithium manganese oxide spinel cathode. J Alloy Compd 618:349–356
23. Armstrong AR, Bruce PG (1996) Synthesis of layered $LiMnO_2$ as an electrode for rechargeable lithium batteries. Nature 381:499–500
24. Yu H, Zhou H (2013) High-energy cathode materials (Li_2MnO_3-$LiMO_2$) for lithium-ion batteries. J Phys Chem Lett 4:1268–1280
25. Zheng F, Ou X, Pan Q, Xiong X, Yang C, Liu M (2017) The effect of composite organic acid (citric acid & tartaric acid) on microstructure and electrochemical properties of $Li_{1.2}Mn_{0.54}Ni_{0.13}Co_{0.13}O_2$ Li-rich layered oxides. J Power Sources 346:31–39
26. Xiang Y, Sun Z, Li J, Wu X, Liu Z, Xiong L, He Z, Long B, Yang C, Yin Z (2017) Improved electrochemical performance of $Li_{1.2}Ni_{0.2}Mn_{0.6}O_2$ cathode material for lithium ion batteries synthesized by the polyvinyl alcohol assisted sol-gel method. Ceram Int 43:2320–2324
27. Song L, Tang Z, Chen Y, Xiao Z, Li L, Zheng H, Li B, Liu Z (2016) Structural analysis of layered Li_2MnO_3-$LiMO_2$ (M=$Ni_{1/3}Mn_{1/3}Co_{1/3}$, $Ni_{1/2}Mn_{1/2}$) cathode materials by Rietveld refinement and first-principles calculations. Ceram Int 42:8537–8544
28. Chen H, Islam MS (2016) Lithium extraction mechanism in Li-rich Li_2MnO_3 involving oxygen hole formation and dimerization. Chem Mater 28:6656–6663
29. Matsunaga T, Komatsu H, Shimoda K, Minato T, Yonemura M, Kamiyama T, Kobayashi S, Kato T, Hirayama T, Ikuhara Y, Arai H, Ukyo Y, Uchimoto Y, Ogumi Z (2016) Structural understanding of superior battery properties of partially Ni-doped Li_2MnO_3 as cathode material. J Phys Chem Lett 7:2063–2067
30. Robertson AD, Bruce PG (2003) Mechanism of electrochemical activity in Li_2MnO_3. Chem Mater 15:1984–1992
31. Oishi M, Yogi C, Watanabe I, Ohta T, Orikasa Y, Uchimoto Y, Ogumi Z (2015) Direct observation of reversible charge compensation by oxygen ion in Li-rich manganese layered oxide positive electrode material, $Li_{1.16}Ni_{0.15}Co_{0.19}Mn_{0.50}O_2$. J Power Sources 276:89–94
32. He Z, Wang Z, Huang Z, Chen H, Li X, Guo H (2015) A novel architecture designed for lithium rich layered $Li[Li_{0.2}Mn_{0.54}Ni_{0.13}Co_{0.13}]O_2$ oxides for lithium-ion batteries. J Mater Chem A 3:16817–16823
33. Boulineau A, Croguennec L, Delmas C, Weill F (2009) Reinvestigation of Li_2MnO_3 structure: electron diffraction and high resolution TEM. Chem Mater 21:4216–4222
34. Matsunaga T, Komatsu H, Shimoda K, Minato T, Yonemura M, Kamiyama T, Kobayashi S, Kato T, Hirayama T, Ikuhara Y, Arai H, Ukyo Y, Uchimoto Y, Ogumi Z (2016) Dependence of structural defects in Li_2MnO_3 on Synthesis temperature. Chem Mater 28: 4143–4150
35. Yu DYW, Yanagida K, Kato Y, Nakamura H (2009) Electrochemical activities in Li_2MnO_3. J Electrochem Soc 156: A417–A424
36. Shin Y, Persson KA (2016) Surface morphology and surface stability against oxygen loss of the lithium-excess Li_2MnO_3 cathode material as a function of lithium concentration. ACS Appl Mater Inter 8:25595–25602
37. Robertson AD, Bruce PG (2002) The origin of electrochemical activity in Li_2MnO_3. Chem Commun 23:2790–2791
38. Nayak PK, Grinblat J, Levi M, Levi E, Kim S, Choi JW, Aurbach D (2016) Al doping for mitigating the capacity fading and voltage decay of layered Li and Mn-rich cathodes for Li-ion batteries. Adv Energy Mater 6:1502398
39. Reimers JN, Fuller EW, Rossen E, Dahn JR (1993) Synthesis and electrochemical studies of $LiMnO_2$ prepared at low temperatures. J Electrochem Soc 140:3396–3401
40. Croy JR, Kim D, Balasubramanian M, Gallagher K, Kang SH, Thackeray MM (2012) Countering the voltage decay in high capacity xLi$_2$MnO$_3$•(1-x)LiMO$_2$ electrodes (M=Mn, Ni, Co) for Li^+-ion batteries. J Electrochem Soc 159:A781–A790
41. Wang D, Li X, Wang Z, Guo H, Xu Y, Fan Y, Ru J (2016) Role of zirconium dopant on the structure and high voltage electrochemical performances of $LiNi_{0.5}Co_{0.2}Mn_{0.3}O_2$ cathode materials for lithium ion batteries. Electrochim Acta 188:48–56
42. Yan G, Li X, Wang Z, Guo H, Wang C (2014) Tris(trimethylsilyl)phosphate: a film-forming additive for high voltage cathode material in lithium-ion batteries. J Power Sources 248:1306–1311
43. Wang R, Li X, Wang Z, Zhang H (2017) Electrochemical analysis graphite/electrolyte interface in lithium-ion batteries: p-

toluenesulfonyl isocyanate as electrolyte additive. Nano Energy 34: 131–140

44. Pan L, Xia Y, Qiu B, Zhao H, Guo H, Jia K, Gu Q, Liu Z (2016) Synthesis and electrochemical performance of micro-sized Li-rich layered cathode material for Lithium-ion batteries. Electrochim Acta 211:507–514
45. Chen C, Chen S, Shui M, Xu X, Zheng W, Feng L, Shu J, Ren Y (2015) Comparative studies on potential dependent electrochemical impedance spectroscopy of cathode material $0.5Li_2MnO_3{\cdot}0.5LiNi_{0.5}Mn_{0.5}O_2$ for the initial two charging cycles. Curr Appl Phys 15: 149–155